

**NICKEL CRYSTALLITE THERMOMETRY**  
**DURING METHANATION**

Douglas K. Ludlow and Timothy S. Cale

Chemical & Bio Engineering Department  
Arizona State University  
Tempe, AZ 85287

**ABSTRACT**

A magnetic method to measure the average temperature of superparamagnetic nickel crystallites has been applied during CO methanation. The method takes advantage of the temperature dependence of the low field magnetization of such catalysts; however, the adsorption of carbon monoxide and the formation of surface carbon species complicate the interpretation of results. Calibrations to account for temperature change and the adsorption of reactants are described. The calibration for the effects of CO is based on the assumption that the interaction of CO with nickel is the same for methanation and disproportionation. Interphase heat transfer calculations based on the thermometric data compare favorably with previous results from ethane hydrogenolysis, and give no indication of microscopic temperature differences between the nickel crystallites and support.

**INTRODUCTION**

The temperature of the active sites is of fundamental importance for the proper interpretation of catalytic kinetics. This information is not currently obtainable; however, a magnetic method to determine the bed average nickel crystallite temperature during ethane hydrogenolysis has been developed in this laboratory (1,2). This paper presents some early results of an effort to extend this magnetic crystallite thermometry to carbon monoxide methanation over nickel catalysts. This system is being studied because of its history, practical importance, more complicated magnetochemistry and higher heat of reaction.

The basis of nickel crystallite thermometry is the temperature dependence of the intrinsic magnetization, or magnetic moment per volume, of nickel crystallites in superparamagnetic samples (1,2,3). This can be determined from low field magnetization data. In order to perform the magnetic thermometry during ethane hydrogenolysis, ethane is introduced into a stream of hydrogen and helium which is flowing through a short catalyst bed. This initiates the exothermic ethane hydrogenolysis reaction. The sample moment decreases rapidly as the bed average nickel crystallite temperature increases. The relationship between sample moment and average crystallite temperature, determined by calibration, is then applied. In addition, any change in moment due to changes in surface coverage must be accounted for (1,2). One of the principle reasons that ethane hydrogenolysis over nickel was the system chosen to demonstrate the magnetic thermometry is that ethane does not affect the magnetic moment of nickel crystallites when hydrogen is present (4,5). However, the introduction of ethane reduces the hydrogen partial pressure slightly, which does affect moment. The moment change due to hydrogen partial pressure change is accounted for as explained elsewhere (2).

A principle conclusion of the research on ethane hydrogenolysis performed to date is the absence of microscopic nickel crystallite to support gradients. In contrast, Matyi, et. al. (6) present evidence for microscopic catalytic crystallite to support temperature differences for CO hydrogenation over iron. The higher heat of reaction for CO hydrogenation certainly makes these gradients more likely than during ethane hydrogenolysis. The presence of any microscopic gradients would interfere with the interpretation of kinetic information; therefore, it is of interest to pursue catalytic crystallite thermometry during methanation. If they are found to exist, then much of the experimental information on CO hydrogenation will have to be reviewed.

In contrast to the simple magnetochemistry found for the ethane hydrogenolysis system, thermometry during methanation is complicated by the fact that carbon monoxide affects the sample moment (7,8) of supported nickel catalysts in a complicated manner. In fact, an understanding of the interaction between CO and nickel is the primary hurdle to overcome in order to perform magnetic thermometry during methanation.

Adsorption and formation of surface species, as well as changes in crystallite size, have an effect on the net magnetization of a nickel catalyst in a fixed field. Therefore, these must be considered in order to perform accurate crystallite thermometry. There have been numerous studies concerned with the nature and role of surface carbon species (carbon and carbides) that form during methanation (4,7-18). The formation of nickel carbonyls, which leads to catalyst deactivation through metal loss and crystallite size changes, has also been studied (19,20).

Using gravimetric analyses, Gardner and Bartholomew (15) found that there was an initial rapid weight gain for the first few minutes after initiating methanation, followed by a more gradual uptake. They concluded that three forms of surface species are present during methanation: (1) easily desorbed species such as CO, CH<sub>4</sub>, H<sub>2</sub>, etc, (2) species reactive with H<sub>2</sub>, such as atomic carbon and (3) unreactive species. Their results also suggest that the species adsorbed after the initial rapid weight gain corresponds to a nonreactive surface species, such as a polymeric carbon. In addition, the weight gain during the initial stages of rapid adsorption decreased with increasing temperature. McCarty and Wise (21), using temperature-programmed surface reaction (TPSR) studies, also reported the formation of two carbon species,  $\alpha$  and  $\beta$ . These correspond to cases 2 and 3 above, respectively.

The interaction of CO with Ni/SiO<sub>2</sub> catalysts has been studied using saturation magnetization methods by Martin et. al. (13), and Mirodotas, et.al. (17), and by low field magnetization techniques by Kuijpers, et.al. (18). Martin et. al. (13), working with samples containing only small amounts of carbon, concluded that the carbon was interstitially dissolved in the nickel lattice. Mirodotas, et. al. (17) and Kuijpers, et. al. (18), using much higher coverages, concluded that there is bulk carbon dissolution and nickel carbidization during CO disproportionation, whereas mainly surface carbidization dominates during methanation. Kuijpers, et. al. (18) also performed static volumetric adsorption analyses between each magnetic measurement. They noted an initial rapid adsorption, followed by a more gradual and linear drop of pressure in their adsorption manifold. The similarity of this result to the observations of Gardner and Bartholomew (15) during methanation is noteworthy. They also noted that the sample magnetization drops to very low levels (up to 90% loss of magnetization) due to bulk carbide formation during disproportionation, whereas the adsorption of hydrogen onto the same samples reduces the relative magnetization by 26% at most.

Since crystallite growth and metal loss would interfere with the magnetic thermometry, it is important to operate in a region where these are minimized. Shen, Dumesic and Hill (19) established a criteria for "safe" operating conditions for methanation over nickel catalysts, where the catalyst no longer deactivated rapidly due to metal loss or particle growth. The criteria is to maintain the equilibrium nickel tetracarbonyl pressure at less than ca.  $7.5 \times 10^{-8}$  Torr. For this work, all experiments were performed in the "safe" operating region. However, because the AC permeameter design currently used can only operate up to a temperature ca. 510 K, conditions were near the "unsafe" operating region. Thus some changes in nickel crystallite size is to be expected. In addition, van Meerten et. al. (20) found nickel crystallite growth during methanation, even though the catalyst was not deactivating dramatically. This indicates a crystallite size dependence on methanation activity. If microscopic crystallite to support temperature gradients exist, then the more active crystallites will be hotter than the less active crystallites. This would further complicate the interpretation of the thermometric results. Conversely, if these gradients do not exist, then a crystallite size effect on activity has little impact on the magnetic thermometry. In that case, the measured temperature is the local temperature of the support and crystallites of all sizes.

## EXPERIMENTAL

A one half gram sample of a 25% nickel on silica catalyst, with an average equivalent spherical diameter of 0.018 cm, was packed into a quartz reactor (22,23) to a bed length of 0.6 cm. The catalyst was from the same batch as the catalysts used in previous crystallite thermometry experiments (1,2). The catalyst sample was reduced in flowing hydrogen at 673 K for 5 hrs and "cleaned" (23) in flowing helium at 723 K for 1/2 hr. Before beginning thermometric experiments, the catalyst was "aged" under reaction conditions until the magnetization no longer changed much. To perform the thermometry, the catalyst sample is initially brought to equilibrium with a flowing stream of hydrogen and helium. The average crystallite temperature is then that of the bulk stream. Reaction is initiated by introducing carbon monoxide at essentially constant total pressure.

An AC permeameter (3,22) is used to follow the changes in magnetic moment of the nickel catalyst sample upon initiation of reaction. The output voltage of the permeameter is related to average catalyst bed temperature via a calibration. Corrections for the change in sample moment due to adsorption and surface species formation are taken into account as described elsewhere in this paper. Reaction products are analyzed using a Carle Analytical gas chromatograph to determine the extent of reaction. Details of the equipment are presented elsewhere (1,2,22). Modifications of the gas handling system which was used for ethane hydrogenolysis were required in order to perform CO methanation. Ultra high purity hydrogen (99.999%, Alphagaz) passes through a palladium Deoxo purifier (Engelhard), a Linde gas purifier column (Model 120: indicating silica gel and molecular sieve), and a 7 micron filter (Nupro) before passing through a Linde mass flowmeter (Model FM 4570). The hydrogen is then mixed with ultra high purity helium (99.999%, Alphagaz) which has similarly passed through a Linde gas purifier column, 7 micron filter, and mass flowmeter. In order to remove remaining components that react with nickel, the hydrogen/helium mixture passes through a Ni/SiO<sub>2</sub> "guard" reactor at 600 K, as well as another silica gel trap. The gas mixture then flows to a manifold where carbon monoxide can be added to the mixture before entering the reactor. The carbon monoxide (99.3%, Air Products) passes through a 7 micron filter and mass flowmeter before passing through a carbonyl trap, which consists of a column of copper turnings (19,20) heated to 500 K. The carbon monoxide is further purified by passing through an Oxy-Trap (Alltech Associates, Inc., Model 4002) heated at 400 K and an Alltech gas purifier column (Model 8125: indicating silica gel and molecular sieve). The carbon monoxide then passes through a needle valve. A ball valve is used to introduce the carbon monoxide into the hydrogen/helium stream just before the sample reactor.

## RESULTS AND DISCUSSION

An example of the rapid decrease in AC permeameter voltage which occurs upon introducing carbon monoxide into the flowing stream of hydrogen and helium is shown in Figure 1. This corresponds to the decrease in sample moment due to the average crystallite temperature rise as well as to the adsorption of carbon monoxide. After this rapid decrease, the sample signal remains relatively constant. When the reaction is terminated by stopping the carbon monoxide flow, there is a rapid increase in sample moment followed by a more gradual increase in moment which levels off within 5 to 10 minutes. This is also shown in Figure 1.

As with ethane hydrogenolysis, the temperature and adsorption calibrations were performed after an initial aging period, in order to minimize any post calibration changes. In order to monitor catalyst aging, a series of methanation experiments was performed with the H<sub>2</sub>/CO ratio kept at 7. Figure 2 shows the decrease in conversion relative to that of the fresh catalyst. The catalyst was left in flowing hydrogen for a period of 16 hours between samples 10 and 11, and for a period of 17 hours between samples 26 and 27. This is taken to account for the higher conversion in run 11; however, there is no corresponding increase between samples 26 and 27. Nevertheless, the activity of the catalyst seems to level off and remain comparatively constant.

The temperature calibration is performed by perturbing the average bed temperature by temporarily removing the catalyst bed from the AC permeameter/oven while flowing hydrogen and helium over the catalyst. After allowing the sample to cool 5 to 10 K, as measured by a thermocouple at the bed exit, the catalyst sample is returned to the optimal sensing location within one of the secondary coils. The AC permeameter signal and exit fluid temperatures are then monitored as the catalyst bed heats. This is repeated several times. The sensitivity (mV/K), determined using least squares regression is assumed constant over the small temperature range considered. As mentioned, this calibration will be affected by changes in crystallite size and by the formation of "permanent" nonmagnetic nickel compounds. Thus, it is important that these do not change significantly between a calibration and the corresponding thermometry experiments.

The calibration procedure used in this study to account for changes in magnetization due to changes in CO uptake takes advantage of the similarity between the uptake results reported during methanation (15) and disproportionation (17,18), discussed previously. The formation of bulk carbide during the CO disproportionation calibration would result in large magnetization decreases and invalidate the procedure; therefore, the possibility of its formation was investigated. Previous studies (17,18) found the formation of bulk carbide during CO disproportionation. However, Mirodatos et. al. (17) using both static and flow experiments, only found bulk carbidization at times greater than 30 minutes for their flow conditions. For experiments in this laboratory, when carbon monoxide is introduced into a helium stream flowing through the catalyst bed, there is a rapid decrease in sample moment, followed by a more gradual decrease in moment, as shown in Figure 3. When disproportionation is allowed to run for longer periods of time, the moment decrease approaches a limiting value after 10 to 15 minutes with a final moment loss of only 6 to 8% of the total sample moment. This relatively small moment loss indicates that no significant amount of bulk carbidization has occurred. When the reaction is terminated, leaving only helium flowing through the catalyst bed, there is a gradual increase in moment which reaches a limiting value after 15 to 20 minutes with a recovery of greater than 90% of the lost moment.

If hydrogen flow is initiated through a catalyst that has previously been exposed to CO disproportionation, there is a rapid increase in sample moment, indicating the removal of a hydrogen reactive surface species. This is in agreement with the results of other laboratories (15,17). There is no discernible change in the sample moment when the hydrogen flow is terminated, leaving only helium flowing. With repeated cycles of 10 minutes of a H<sub>2</sub>/He mixture followed by 20 minutes of pure He flow through the catalyst bed, there is a rapid increase in sample moment after each hydrogen introduction. However, the magnitude of the moment increase declines somewhat with each successive initiation of hydrogen flow. Analysis of the effluent shows that methane is evolved after each hydrogen introduction. Similar results are also obtained for the catalyst after methanation with an H<sub>2</sub>/CO ratio of at least seven. There is no marked difference in the response of the sample moment to the initiation of hydrogen flow after either the methanation or disproportionation experiments. These results indicate the formation of carbon species, during both methanation and disproportionation, all forms of which are not available for reaction with hydrogen, but with which they become available for reaction. This corresponds to the interstitially dissolved carbon reported by other researchers (13,17,18), where the surface carbon is removed by the hydrogen, and is replaced by the migration of the interstitially dissolved carbon.

The use of CO disproportionation for a calibration to account for carbon monoxide adsorption effects is substantiated by these results because: (1) they indicate no significant formation of bulk carbide, at least not in the short time required for the calibrations, and (2) they indicate that there is no significant difference in the carbon formed during both methanation and disproportionation. The results do not preclude the possibility of the formation of the filamentous carbon species reported by other researchers (24-26) during the CO disproportionation calibration. Such filamentous carbon species can deactivate the catalyst, but have no effect on the sample moment (18).

Baseline drift is usual when using an AC permeameter. Therefore for thermometry, we rely on the rapid change in sample moment which occurs within the first 1/2 to 1 minute after introducing carbon monoxide into the hydrogen and helium stream. As mentioned, there is also a rapid decrease in sample moment when carbon monoxide is introduced into a helium stream (see Figure 3). The magnitude of the rapid decrease depends upon the carbon monoxide partial pressure, and is reproducible. This is in apparent agreement with the results of Gardner and Bartholomew (15) and Kuijpers et.al. (18). For calibration purposes, this magnitude is assumed to correspond to the adsorption of carbon monoxide which occurs upon the initiation of methanation. The calibration is performed by introducing carbon monoxide at various partial pressures into helium. The carbon monoxide is allowed to flow only long enough to record the initial rapid decrease in sample moment (2 to 3 minutes). The results were fit to the following equation using least squares regression:

$$\Delta \text{Signal (mV)} = 0.00462 * (P_{\text{CO}} \text{ (Torr)})^{0.662} \quad 1)$$

As indicated, with the termination of methanation there is a rapid increase in moment within the first minute after the carbon monoxide flow is stopped, which is followed by a more gradual increase. However, when the carbon monoxide flow is stopped during CO disproportionation there is only a gradual increase in sample moment, as shown in Figure 3. In the absence of a rapid moment change, a time of 60 seconds was arbitrarily chosen to represent the signal increase corresponding to desorption upon reaction termination. Again, the change is reproducible, and dependent upon the carbon monoxide partial pressure present before reaction termination. The results with this choice of time scale is represented by the equation

$$\Delta \text{Signal (mV)} = 0.00071 * (P_{\text{CO}} \text{ (Torr)})^{1.05} \quad 2)$$

obtained using least squares regression.

The introduction of carbon monoxide in order to initiate methanation slightly decreases the hydrogen partial pressure, which effects the sample moment. A calibration for the moment change due to hydrogen partial pressure changes is performed by slightly changing the hydrogen partial pressure during reaction. Hydrogen partial pressure affects the reaction rate, however for the small changes that are required for the calibration, the extent of conversion changes at most only 2 to 5%. A small decrease in signal results from a decrease in hydrogen partial pressure. Just the opposite was observed if the hydrogen partial pressure was changed during ethane hydrogenolysis (2). Thus, it seems that the decrease in hydrogen partial pressure leads to an increase in the crystallite surface coverage by carbon, instead of a decrease in surface coverage by hydrogen. The moment change is reproducible and dependent upon the change in hydrogen partial pressure. There is no significant difference in the magnitude of the moment decrease with decreasing partial pressure and the moment increase with an equivalent increase in hydrogen partial pressure. The results are correlated using least squares regression and fit to the equation

$$\Delta \text{Signal (mV)} = 0.00003 (\Delta P_{\text{H}} \text{ (Torr)})^{1.27} \quad 3)$$

It is important to note that this effect is one to two orders of magnitude less than that for changes in carbon monoxide partial pressure, and seldom has significance in the thermometry experiments since the hydrogen partial pressure changes only slightly.

The average crystallite temperature rise due to the initiation of methanation is determined by first measuring the magnitude of the signal change upon the initiation of reaction. Signal changes due the increase in CO partial pressure and decrease in hydrogen partial pressure are then subtracted. The result is then divided by the temperature sensitivity (mV/K) to determine the temperature rise.

The validity of the calibration technique was tested by comparing the results of this study with the those for ethane hydrogenolysis. Assuming that no microscopic crystallite to support gradients exist, it is possible to determine the interphase Nusselt number using the described thermometry (1,2,27,28). The average crystallite temperature rise determined from crystallite thermometry is used to calculate the average solid temperature. This information, along with the average bulk fluid temperature rise, and the conversion (heat release) allows the direct

calculation of interphase Nusselt number within the differential reactor assumption. The flow conditions ( $0.3 < \text{Re} < 0.6$ ) were not varied enough in this study to determine the functional dependence of the interphase Nusselt number (Nu) on Reynolds number (Re). The interphase Nu was determined for runs for which the catalyst bed was operated under differential conditions, taken as less than 5% conversion. The resulting Nu are scattered uniformly around the results from the previous study using ethane hydrogenolysis (2,27,28). The average Nu determined from the methanation data matches the previously determined relationship. If the results obtained during ethane hydrogenolysis are accepted, then the calibration method used in this work seems valid. Due to the limited Re range covered, these preliminary results are inconclusive, but also indicate the absence of microscopic temperature differences between the crystallite and support. A significantly smaller interphase Nu would be expected if these microscopic temperature differences existed. If this conclusion is correct, then any crystallite size dependence of activity does not interfere with the thermometry.

The possibility of crystallite growth during the initial aging period was investigated. This is not critical to this work, but it is of interest. Samples with larger nickel crystallites exhibit a larger magnetization than those with smaller crystallites, at a fixed field (3). As discussed, the calibrations were performed on the "aged" catalyst. Therefore, the sample moment would be larger than that for the fresh sample, at a given field, if crystallite growth occurred. This assumes that there is no significant loss of nickel. Thus, the fresh catalyst would show smaller magnetization changes than the aged sample for a given temperature change. Therefore, if the temperature calibration performed on the aged sample is applied, a smaller "measured" solid temperature rise is indicated from crystallite thermometry. The average solid temperature rise expected for given flow and conversion data can be estimated using the interphase heat transfer data from the ethane hydrogenolysis study (2,27,28). As discussed above, the interphase heat transfer results using data gathered on the aged catalyst have already been shown to agree with these previous results. Figure 4 shows a plot of the difference between the "measured" solid temperature and the "predicted" temperature during the initial aging period. The results show that initially, the "measured" solid temperatures were much smaller than that predicted. The difference between the measured and predicted temperatures decreased as the catalyst aged. Subsequent data reflects scatter. The crystallite growth inferred from these results is in agreement with the results of van Meerten et. al. (20). Those researchers performed crystallite size estimates as the catalyst aged and found crystallite growth. However, contrary to the results of that laboratory, a significant loss of activity was found in this work. A strong size dependence of activity is not apparent.

### CONCLUSIONS

Nickel crystallite thermometry has been performed during CO methanation. The analysis and calibrations are more complicated than for ethane hydrogenolysis, because of the more complicated magnetochemistry involved. The calibration scheme used to account for CO adsorption and the formation of surface species seems to work satisfactorily. The scheme used is based on results that show no significant formation of bulk carbide during the disproportionation calibration and no significant difference in the carbon species formed during methanation and disproportionation. In addition, interphase Nusselt number estimates are in good agreement with those obtained during ethane hydrogenolysis. However, it would be more satisfying to have a calibration based on methanation, rather than disproportionation.

An alternate calibration scheme in which the methanation rate is decreased while maintaining the same CO adsorption conditions is under development. The approach is to decrease the reaction rate while holding the adsorption/surface carbon species formation effects constant. The effect due to the temperature rise will decrease. Thus, it should be possible to extrapolate to zero rate in order to isolate the moment change due only to adsorption. Preliminary results following

this line of reasoning are inconclusive, and further work is necessary to determine whether such a calibration scheme can be developed.

#### ACKNOWLEDGEMENTS

Financial assistance from the Petroleum Research Fund and the National Science Foundation is gratefully acknowledged.

#### REFERENCES

1. Cale, T. S., and Ludlow, D. K., J. Catal. **86**, 450 (1984).
2. Cale, T. S., J. Catal. **90**, 40 (1984).
3. Selwood, P. W., "Chemisorption and Magnetization" Academic Press, New York, 1975.
4. Martin, G. A., and Imelik, B., Surf. Sci. **42**, 157 (1974).
5. Martin, G. A., Dutarte, R., and Dalmon, J. A., in "Growth of Properties of Metal Clusters", Bourdon, J. (ed.) p. 467, Elsevier, Amsterdam, 1980.
6. Matyi, R. J., Butt, J. B., and Schwartz, L. H., J. Catal. **91**, 185 (1985).
7. Geus, J. W., Nobel, A. P. P., and Zwietering, P., J. Catal. **1**, 8 (1962).
8. Primet, M., Dalmon, J. A., and Martin, G. A., J. Catal. **46**, 25 (1977).
9. Mulay, L. N., Everson, R. C., Mahajan, O. P., and Walker, P. L., Jr., AIP Conf. Proc., **29** (Magn. Magn. Mater., Annu. Conf., 21st), 536 (1975).
10. Farrauto, R. J., J. Catal. **41**, 482 (1976).
11. Wentrcek, P. R., Wood, B. J., and Wise, H., J. Catal. **43**, 363 (1976).
12. Martin, G. A., Dalmon, J. A., and Primet, M., C. R. Hebd. Seances. Acad. Sci. SerC. **284**(4), 163 (1977).
13. Martin, G. A., Primet, M., and Dalmon, J. A., J. Catal. **53**, 321 (1978).
14. Falconer, J. L., and Zagli, A. E., J. Catal. **62**, 280 (1980).
15. Gardner, D. C., and Bartholomew, C. H., Ind. Eng. Chem. Fundam. **20**, 229 (1981).
16. Kuijpers, E. G. M., Breedjik, A. K., van der Wal, W. J. J., and Geus, J. W., J. Catal. **81**, 429 (1983).
17. Mirodatos, C., Dalmon, J. A., and Martin, G. A., Stud. Surf. Sci. Catal. **19**, 505 (1984).
18. Kuijpers, E. G. M., Kock, A. J. H. M., Nieuwesteeg, M. W. C. M. A., and Geus, J. W., J. Catal. **95**, 13 (1985).
19. Shen, W. M., Dumesic, J. A., and Hill, C. G., Jr., J. Catal. **68**, 152 (1981).
20. van Meerten, R. Z. C., Beaumont, A. H. G. M., van Nisselrooij, P. F. M. T., and Coenen, J. W. E., Surf. Sci. **135**, 565 (1983).
21. McCarty, J. C., and Wise, H., J. Catal. **57**, 406 (1979).
22. Cale, T. S., and Ludlow, D. K., Anal. Instrum. **13**(2), 183 (1984).
23. Cale, T. S., and Richardson, J. T., J. Catal. **79**, 378 (1983).
24. Rostrup-Nielsen, J. R., J. Catal. **27**, 343 (1972).
25. Tøttrup, P. B., J. Catal. **29**, (1976).
26. Gardner, D. C., and Bartholomew, C. H., Ind. Eng. Chem. Prod. Res. Dev. **20**, 80 (1981).
27. Lawson, J. M., Ludlow, D. K., and Cale, T. S., Proceedings IASTED International Conference, AIMS '84, 26 (1984).
28. Cale, T. S., and Lawson, J. M., Chem. Eng. Commun. **39**, 241 (1985).

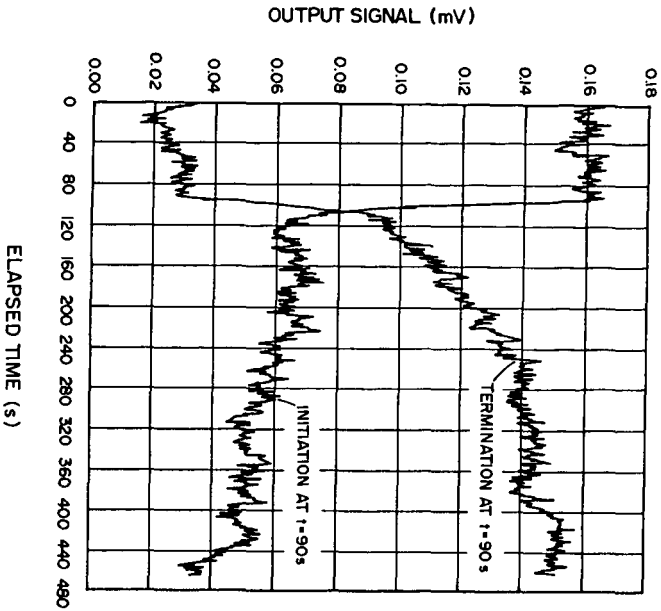


Figure 1. Examples of the changes in AC permeameter output voltage that occur upon the initiation and termination of CO methanation.

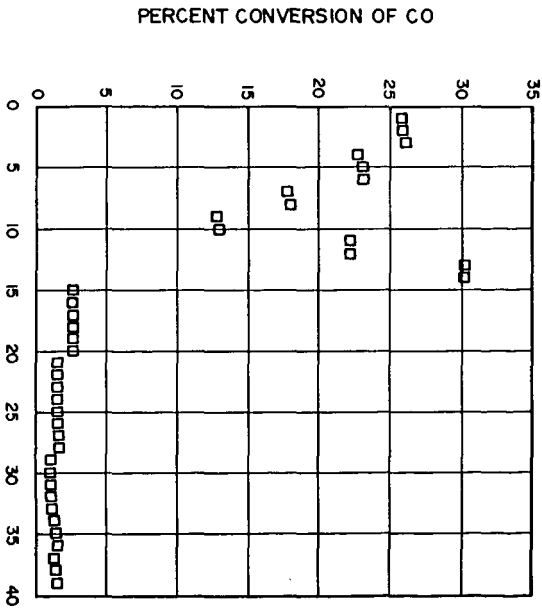


Figure 2. Conversion data during initial aging period. The  $H_2/CO$  ratio is seven. The catalyst was left in flowing hydrogen for 16 and 17 hours between samples 10-11 and 26-27, respectively.

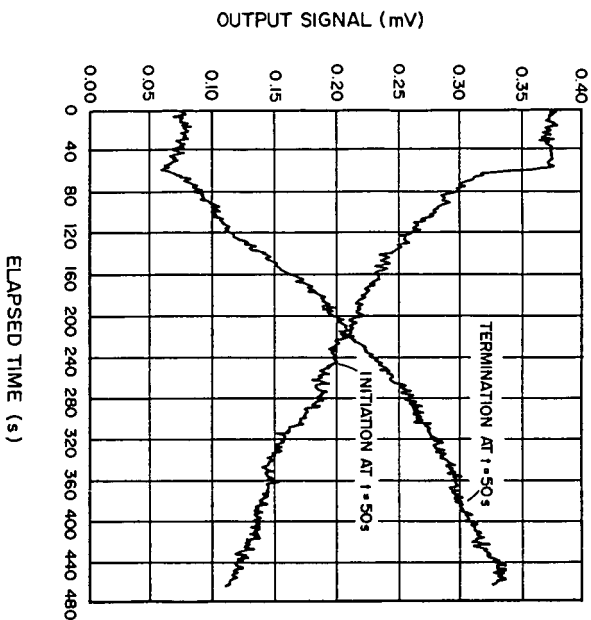


Figure 3. Examples of the changes in AC permeameter output voltage that occur upon the initiation and termination of CO disproportionation. (See text for explanation.)

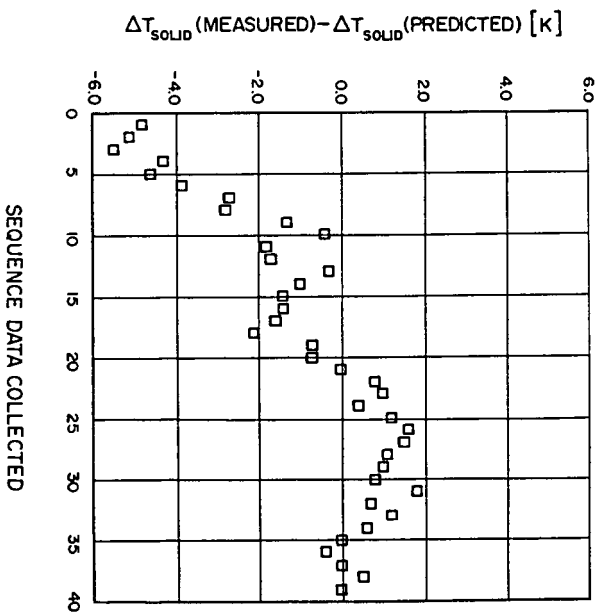


Figure 4. Difference in the "predicted" and "measured" solid temperature rise during initial aging period. (See text for explanation.)